AFOSR TR-81-0152

PSI-TR-244

# LEVEL II

③

SC

⑥ TURBULENT BOUNDARY LAYER HEAT TRANSFER.

⑨ ANNUAL REPORT. 1 Nov 79 - 31 Oct 80

Effect of Surface Roughness Character
on Turbulent Boundary Layer Heating

by

⑩ M. L. Finson, A. S. Clarke and P. K. S. Wu

⑪ Jan 81

⑫ 46

Sponsored by

Air Force Office of Scientific Research (AFSC)
United States Air Force

Under Contract No. F49620-80-C-0015

⑮ ⑯ 2307 ⑰ A1

(17) 933 8600

# PHYSICAL SCIENCES INC.
30 COMMERCE WAY, WOBURN, MASS. 01801

391105

81 3 16 012

AD A096381

ACKNOWLEDGEMENT

| REPORT DOCUMENTATION PAGE | READ INSTRUCTIONS BEFORE COMPLETING FORM |
|---|---|

| 1. REPORT NUMBER | 2. GOV ACCESSION NO. | 3. RECIPIENT'S CATALOG NUMBER |
|---|---|---|
| AFOSR-TR- 81-0152 | AD-A096381 | |

| 4. TITLE (and Subtitle) | 5. TYPE OF REPORT & PERIOD COVERED |
|---|---|
| Turbulent Boundary Layer Heat Transfer | Interim 11/1/79 – 10/31/80 |
| | 6. PERFORMING ORG. REPORT NUMBER TR-244 |

| 7. AUTHOR(s) | 8. CONTRACT OR GRANT NUMBER(s) |
|---|---|
| M. L. Finson, A. S. Clarke, P. K. S. Wu | F49620-80-C-0015 |

| 9. PERFORMING ORGANIZATION NAME AND ADDRESS | 10. PROGRAM ELEMENT, PROJECT, TASK AREA & WORK UNIT NUMBERS |
|---|---|
| PHYSICAL SCIENCES INC. 30 Commerce Way Woburn, MA 01801 | 61102F / 2307/A1 |

| 11. CONTROLLING OFFICE NAME AND ADDRESS | 12. REPORT DATE |
|---|---|
| Air Force Office of Scientific Research /NA Bolling AFB, D.C. 20332 | January 1981 |
| | 13. NUMBER OF PAGES 45 |

| 14. MONITORING AGENCY NAME & ADDRESS(if different from Controlling Office) | 15. SECURITY CLASS. (of this report) |
|---|---|
| | Unclassified |
| | 15a. DECLASSIFICATION DOWNGRADING SCHEDULE |

16. DISTRIBUTION STATEMENT (of this Report)

Approved for public release; distribution unlimited

17. DISTRIBUTION STATEMENT (of the abstract entered in Block 20, if different from Report)

18. SUPPLEMENTARY NOTES

19. KEY WORDS (Continue on reverse side if necessary and identify by block number)

Turbulent Boundary Layers
Turbulent Heat Transfer
Re-entry Heating

20. ABSTRACT (Continue on reverse side if necessary and identify by block number)

A Reynolds stress model for turbulent boundary layers is used to study surface roughness effects on skin friction and heat transfer. The issues of primary interest are the influence of roughness character (element shape and spacing) and the nature of roughness effects at high Mach numbers. Computations based on the model compare satisfactorily with measurements from experiments involving variations in roughness character, in low speed and modestly supersonic conditions. The more limited data base at hypersonic Mach numbers

DD FORM 1473 1 JAN 73    EDITION OF 1 NOV 65 IS OBSOLETE    UNCLASSIFIED

is also examined with reasonable success, although no quantitative explanation is offered for the reduction of heat transfer with increasing roughness observed by Holden at $M_{(e)} = 9.4$.

The present calculations indicate that the mean velocity is approximately uniform over much of the height range below the tops of the elements, $y < k$. With this constant "roughness velocity," it is simple to estimate the form drag on the elements. This roughness velocity has been investigated by systematically exercising the present model over ranges of potential parameters. The roughness velocity is found to be primarily a function of the projected element frontal area per unit surface area, thus providing a new and simple method for predicting roughness character effects. The model further suggests that increased boundary layer temperatures should be generated by roughness at high edge Mach numbers, which would tend to reduce skin friction and heat transfer, perhaps below smooth wall levels.

ABSTRACT


A Reynolds stress model for turbulent boundary layers is used to study surface roughness effects on skin friction and heat transfer. The issues of primary interest are the influence of roughness character (element shape and spacing) and the nature of roughness effects at high Mach numbers. Computations based on the model compare satisfactorily with measurements from experiments involving variations in roughness character, in low speed and modestly supersonic conditions. The more limited data base at hypersonic Mach numbers is also examined with reasonable success, although no quantitative explanation is offered for the reduction of heat transfer with increasing roughness observed by Holden at $M_e$ = 9.4.

The present calculations indicate that the mean velocity is approximately uniform over much of the height range below the tops of the elements, $y \leq k$. With this constant "roughness velocity," it is simple to estimate the form drag on the elements. This roughness velocity has been investigated by systematically exercising the present model over ranges of potential parameters. The roughness velocity is found to be primarily a function of the projected element frontal area per unit surface area, thus providing a new and simple method for predicting roughness character effects. The model further suggests that increased boundary layer temperatures should be generated by roughness at high edge Mach numbers, which would tend to reduce skin friction and heat transfer, perhaps below smooth wall levels.

TABLE OF CONTENTS

LIST OF ILLUSTRATIONS

## LIST OF TABLES

# I. INTRODUCTION

Surface roughness plays an important role in turbulent boundary layer skin friction and heat transfer for many high-speed flight applications. Although the general nature of roughness effects for typical types of "sand grain" roughness has been known for many years, dating back to the classic study by Nikuradse,[1] modern composite materials introduce a different character of roughness. By roughness character, we mean the shape, spacing and perhaps the distribution of roughness heights. With a woven composite material, for example, the exposed fibers would be approximately cylindrical in shape, in contrast to the more nearly hemispherical or pyramidal shape of conventional roughness elements.

Previous studies of roughness character have been somewhat limited experimentally, and the only theoretical investigations have been quite empirical. Schlichting[2] measured the drag due to various element shapes (spheres, spherical segments, cones) at several relative spacings on the side wall of a water channel. There are several reported experiments involving two-dimensional roughness elements (machined grooves normal to the flow direction). Some years ago, Bettermann[3] correlated the available data to obtain $k_s/k$, the ratio of the effective sand grain roughness height to the actual roughness height, as a function of roughness shape and spacing. Of course, the effective sand grain roughness can be used in Nikuradse's results to predict the skin friction increase. Dvorak[4] has applied Betterman's data to practical heating applications. Unfortunately, much of the data that had previously been correlated were obtained on two-dimensional roughness patterns. One might expect a difference in the nature of the flow over 2-D versus 3-D roughness. For example, with 2-D roughness, the flow would be more likely to separate, resulting in a cavity flow in the grooves between the elements. The three-dimensional case is of far greater practical importance, and the 2-D type of roughness will not be considered further here.

A second important issue concerns the nature of roughness effects in supersonic flow conditions. Density variations could alter the extent of roughness-induced augmentation of friction or heating, and the character of the flow about the elements might change if supersonic conditions prevail locally. Only recently have measurements started to become available on supersonic and hypersonic rough-wall boundary layers, .offering an opportunity to examine the Mach number issue in a preliminary fashion.

In this study we employ a Reynolds stress turbulent boundary layer model which specifically accounts for roughness effects. Roughness is represented by distributed sources and sinks in the various governing equations. The most important term is a sink term in the mean momentum equation representing form drag on the roughness elements. In previous studies,[5] the approach was developed and compared against subsonic rough wall boundary layer measurements. The present objective is to apply the theory to variations in roughness character, as well as to supersonic conditions. A model extension to treat closely packed roughness elements will be described. Calculations will be compared with a variety of data to establish confidence in the model; then, the model will be exercised systematically over a range of parameters to develop a scaling law for roughness character that is simple and quite different from existing approaches.

## II.  ROUGH WALL TURBULENCE MODEL

The turbulence model used here  is one in which closure approxima-
tions are applied at second order.  With the exception of the treatment
of roughness, the formulation is somewhat standard at this time, and has
been successfully applied to a variety of smooth wall boundary layer and
free shear flows.  The model accounts for both mean and fluctuating velo-
cities and temperatures.  The dependent velocity variables are the mean
velocity vector $U_i$, the Reynolds stress tensor $\overline{u_i' u_j'}$, and the isotropic
dissipation rate $\Phi$.  The analogous thermal variables (temperature or,
more precisely, enthalpy h) are the mean enthalpy $\bar{h}$, the mean square fluc-
tuating enthalpy $\overline{h'^2}$, and the Reynolds heat flux vector $\overline{u_i'h'}$.  Under
the boundary layer approximation, this set of variables reduces to U,
V, $\overline{u'^2}$, $\overline{v'^2}$, $\overline{w'^2}$, $\overline{u'v'}$, $\Phi$, $\bar{h}$, $\overline{h'^2}$, $\overline{u'h'}$, and $\overline{v'h'}$.  The development of
the governing equations and the required closure approximations are de-
scribed in Ref. 5 and will not be repeated here.  The actual equations
are given in the Appendix.

The effect of roughness is described by distributed source or
sink terms in the appropriate equations.  As already noted, only distri-
buted roughness is considered here, and we make the fundamental assumption
that the flow around individual elements is attached to the elements.
For two-dimensional roughness, the flow might be treated more appropriately
as cavity flows between the elements.  In the present model, roughness
elements provide a distributed sink (due to drag) for mean momentum, and
distributed sources for mean turbulent kinetic energy and dissipation.
We idealize the rough surface as being made up of identical elements (al-
though the extension to a size distribution is feasible).  The bottom of
the elements corresponds to y = 0.  Let k be the element height, D(y) be
the element diameter at height y (for $0 \leq y \leq k$), and $\ell$ be the average
center-to-center element spacing.  The functional form of the diameter
D(y) is easily prescribed for simple shapes such as cones or hemispheres.
As discussed in Ref. 5 and in the Appendix, the drag on the elements per
unit volume is the appropriate sink term in the equation for the mean
velocity:

$$R_u = -\frac{1}{2} \rho U^2 C_D D(y)/\ell^2 . \qquad (1)$$

A drag coefficient value of $C_D = 0.6$ is roughly appropriate for elements such as cones or hemispheres. The source terms for kinetic energy and dissipation, which are less important numerically, are given in the Appendix. Except in the Stokes flow regime, heat transfer to an element should be small. Therefore, the only roughness term appearing in the thermal equations is a source for the mean static enthalpy. This term is simply constructed so that, in combination with Eq. (1), form drag does not alter total enthalpy:

$$R_h = +\frac{1}{2} \rho U^3 C_D D(y)/\ell^2. \qquad (2)$$

In the approach that we have just outlined, roughness elements are assumed to occupy no physical space. This assumption becomes progressively worse as the roughness density increases. Accordingly, the model has been extended to account for the blockage effect of the roughness elements. This is done in a simple manner. At a given height y, the fraction of the flow area in the x direction, that is open to the flow, is $1 - D(y)/\ell$; terms that act in the streamwise direction, such as the convective operator $\rho u \, \partial/\partial x$, are multiplied by this factor. Terms that act on a surface area whose normal is in the y direction, or that act on a unit volume, should be multiplied by $1 - \pi D^2/4\ell^2$. However, the distributed roughness source or sink terms are already based on the total volume, rather than available flow volume, and need no such factor. If the entire equation is divided by $B(y) = 1 - \pi D^2/4\ell^2$, a relatively simple change occurs. For example, the mean momentum equation becomes

$$f(y) \rho U \frac{\partial U}{\partial x} + \rho V \frac{\partial U}{\partial y} = - f(y) \frac{\partial p}{\partial x} + \frac{1}{B} \frac{\partial}{\partial y} B\mu \frac{\partial U}{\partial y} .$$

$$(3)$$

$$- \frac{\partial}{\partial y} (\overline{\rho u'v'}) - \frac{1}{2} \rho U^2 C_D \frac{D}{\ell^2} B^{-1}$$

where

$$f(y) = \frac{1 - D/\ell}{1 - \pi D^2/4\ell^2} \quad .$$

(4)

The function $f(y)$ contains the main effect of blockage and may be handled by merely redefining the standard stream function which is used to eliminate the normal velocity.

$$\frac{\partial \psi}{\partial y} = f(y) \rho U , \qquad \frac{\partial \psi}{\partial x} = - \rho V.$$

(5)

Note that if the elements are packed so tightly that they are touching over some range of y, then $D = \ell$ and $f(y) = 0$. The stream function would be forced to be independent of y over that range (from Eq. (5)); the velocity would remain zero from the bottom of the elements up to the height where $D < \ell$ and flow is unblocked. Of course, common sense would dictate redefining y = 0 as the lowest point where the flow is unblocked. However, the model does yield the limiting result that U = 0 if there is no space between the elements.

A major advantage of the present Reynolds stress model is that solutions are obtained for both velocity and thermal variables. Heat transfer is obtained directly, without invoking a Reynolds analogy. Finite difference solutions are obtained using the obvious boundary conditions: fluctuating quantities are zero at the solid wall and in the free stream. It is important to note that the boundary conditions at the wall are not treated as empirical functions of roughness as has been done in other approaches.[6] For numerical solutions, the equations are first transformed to the stream function coordinate, guaranteeing mass conservation and eliminating the normal velocity V. The transverse coordinate is normalized by the edge value of the stream function, so that additional mesh points need not be carried in the free stream to allow for boundary layer growth. For proper resolution of the region near the wall, a linear mesh in the logarithm of the stream function is used. The finite-difference equations are solved with a block tridiagonal Newton-Raphson technique.

### III. COMPARISON WITH EXPERIMENTS ON ROUGHNESS CHARACTER

The first measurements to be examined are those of Schlichting,[2] which were obtained in a 4 cm x 17 cm water channel. Various arrangements of roughness elements, shown in Fig. 1, were used on the wall. Velocity profiles were measured, and the skin friction or equivalent sand grain roughness $k_s$ was derived from the logarithmic portion of the profile. The simple shapes and regular spacing of the roughness elements can be simulated quite well by our roughness model, with the exception of the short angles, which were not investigated.

Figure 2 compares the skin friction computed with our model against Schlichting's data for the spherical segments. As indicated in Fig. 1, the segments are nearly hemispherical (height = 0.26 cm, radius = 0.40 cm). Further, the dashed lines were not actually presented by Schlichting.[2] He determined the equivalent sand grain roughness, based on the observed increase in $C_f$ over the smooth wall value at selected downstream stations. We took the liberty of using the $k_s$ values to obtain the augmentation of $C_f$ as a function of distance. In so doing, the appropriate upstream initial conditions are ignored. The computations were started with a fully turbulent smooth wall boundary layer at $x/\ell = 0.03$. Given the arbitrary treatment of initial conditions, the mild disagreement at upstream locations is not significant. Otherwise, the model reproduces fairly well the observed increase in skin friction with increasing roughness density.

A detailed comparison of the mean velocity profiles computed from the present model with Schlichting's data for spherical segments is shown in Fig. 3, in semi-logarithmic coordinates ($U_\tau = \sqrt{\tau_w/\rho_w}$). Agreement is again seen to be quite good, with a 10-15% error for the most dense packing. The data and curves of Fig. 3 agree well with the velocity profile of classic rough wall pipe flow when replotted against $y/k_s$.

Figure 4 shows the computed skin friction coefficients and Schlichting's measurements for three different element shapes as a function of spacing. The calculations were evaluated at $Re_x \approx 10^7$, but the increase in skin
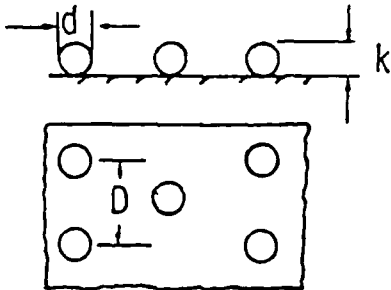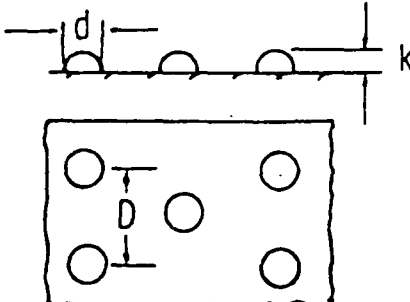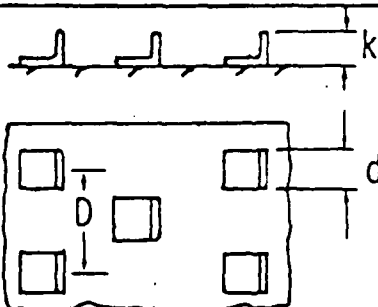
| Roughness Elements | Dimension | D cm | d cm | k cm | $k_s$ cm |
|---|---|---|---|---|---|
| Spheres |  | 4 | .41 | .41 | .093 |
| | | 2 | .41 | .41 | .344 |
| | | 1 | .41 | .41 | 1.26 |
| | | .6 | .41 | .41 | 1.56 |
| | | 1 | .21 | .21 | .172 |
| | | .5 | .21 | .21 | .759 |
| Spherical Segments |  | 4 | 0.8 | 0.26 | .031 |
| | | 3 | 0.8 | 0.26 | .049 |
| | | 2 | 0.8 | 0.26 | .149 |
| Cones |  | 4 | 0.8 | .375 | .059 |
| | | 3 | 0.8 | .375 | .164 |
| | | 2 | 0.8 | .375 | .374 |
| Short-angles |  | 4 | 0.8 | 0.30 | .291 |
| | | 3 | 0.8 | 0.30 | .618 |
| | | 2 | 0.8 | 0.30 | 1.47 |

Fig. 1  Schlichting roughness experiments.[2]
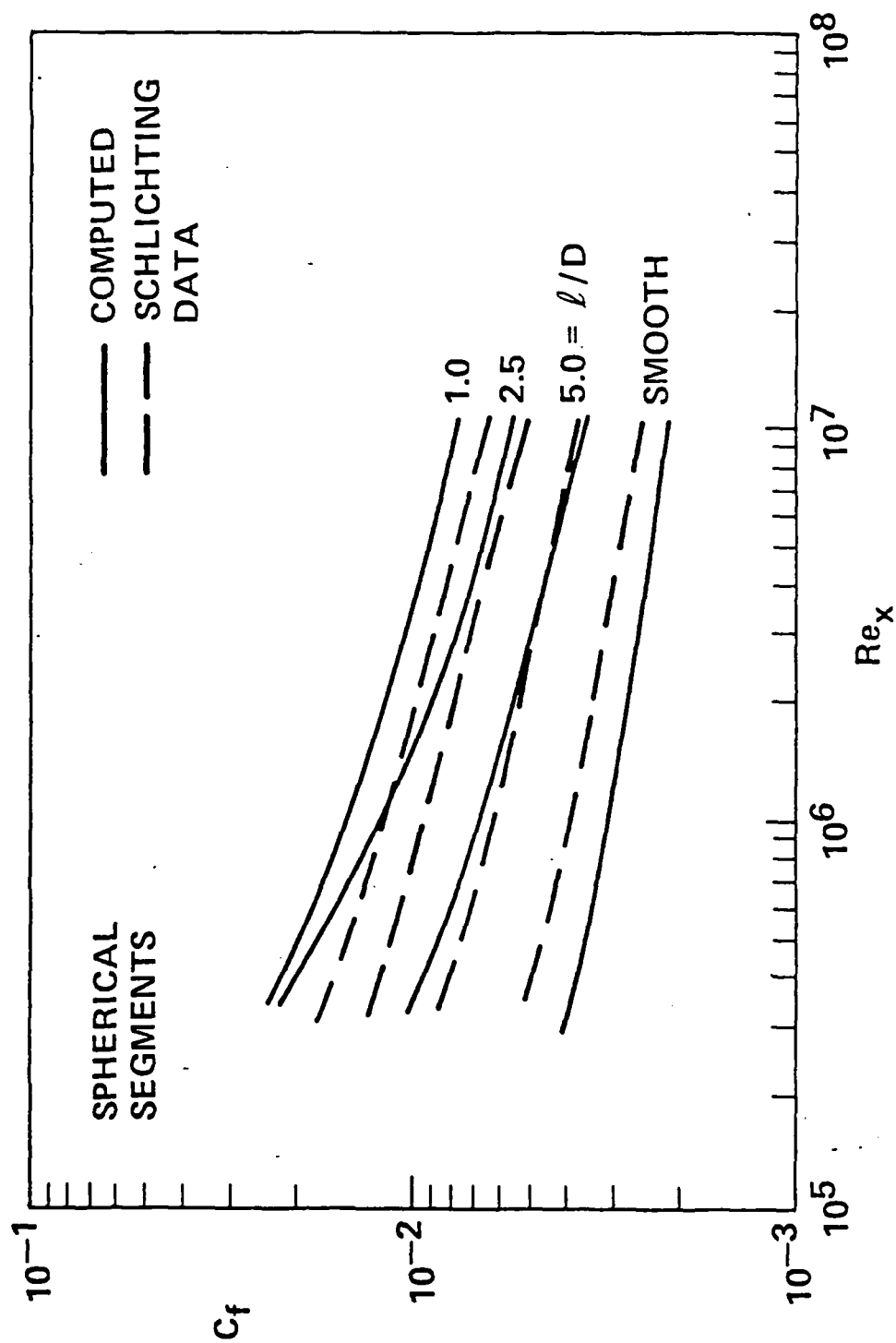
Fig. 2 Computed and measured skin friction coefficients vs. distance Reynolds number, as a function of roughness spacing for spherical segments ($\cong$ hemispheres).

Fig. 3   Computed mean velocity profiles compared to Schlichting[2] measurements for spherical segments at three relative spacings.

Fig. 4 Comparison of calculated skin friction augmentation vs. Schlichting experimental results,[2] as a function of roughness spacing for three types of elements.

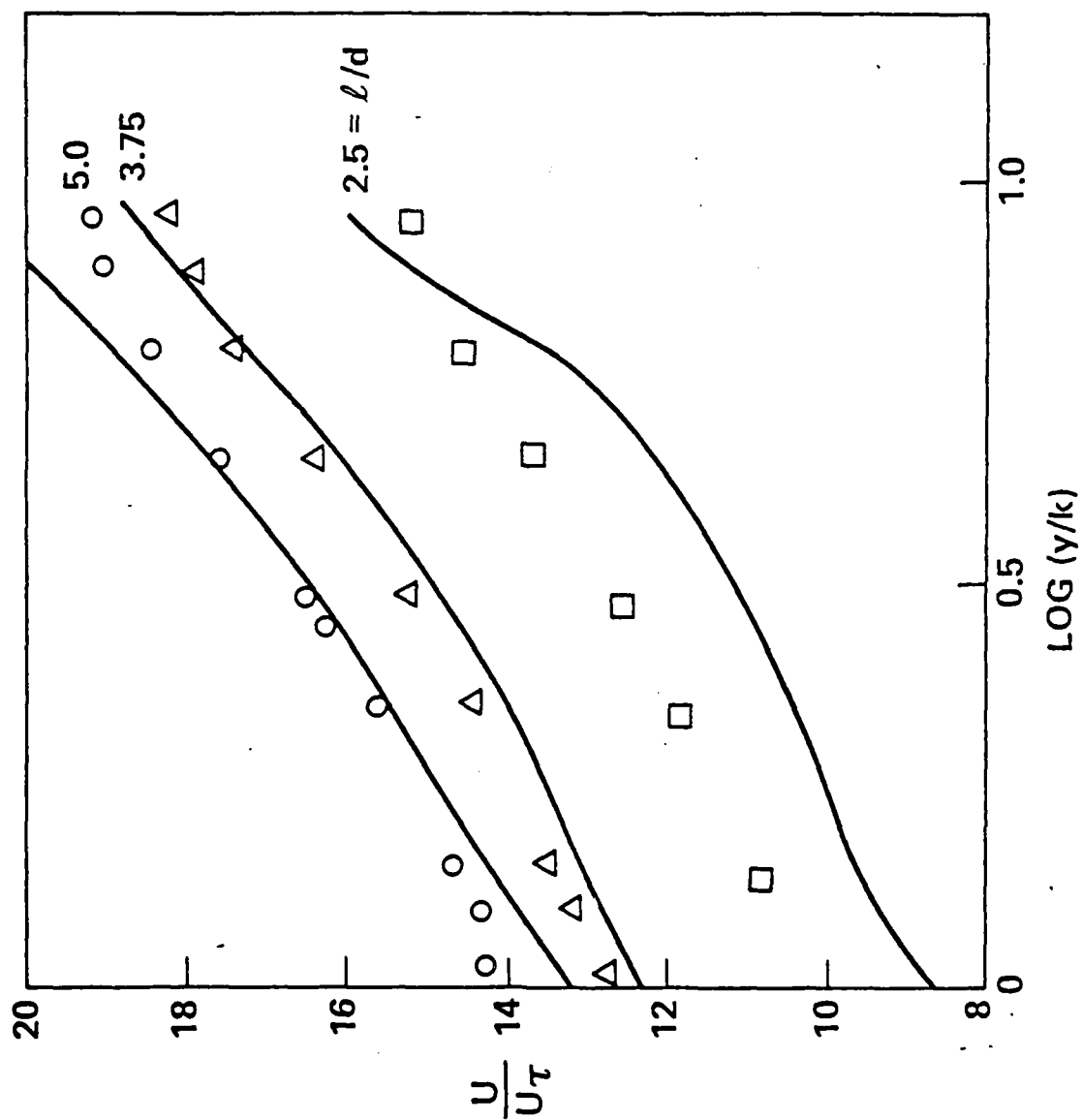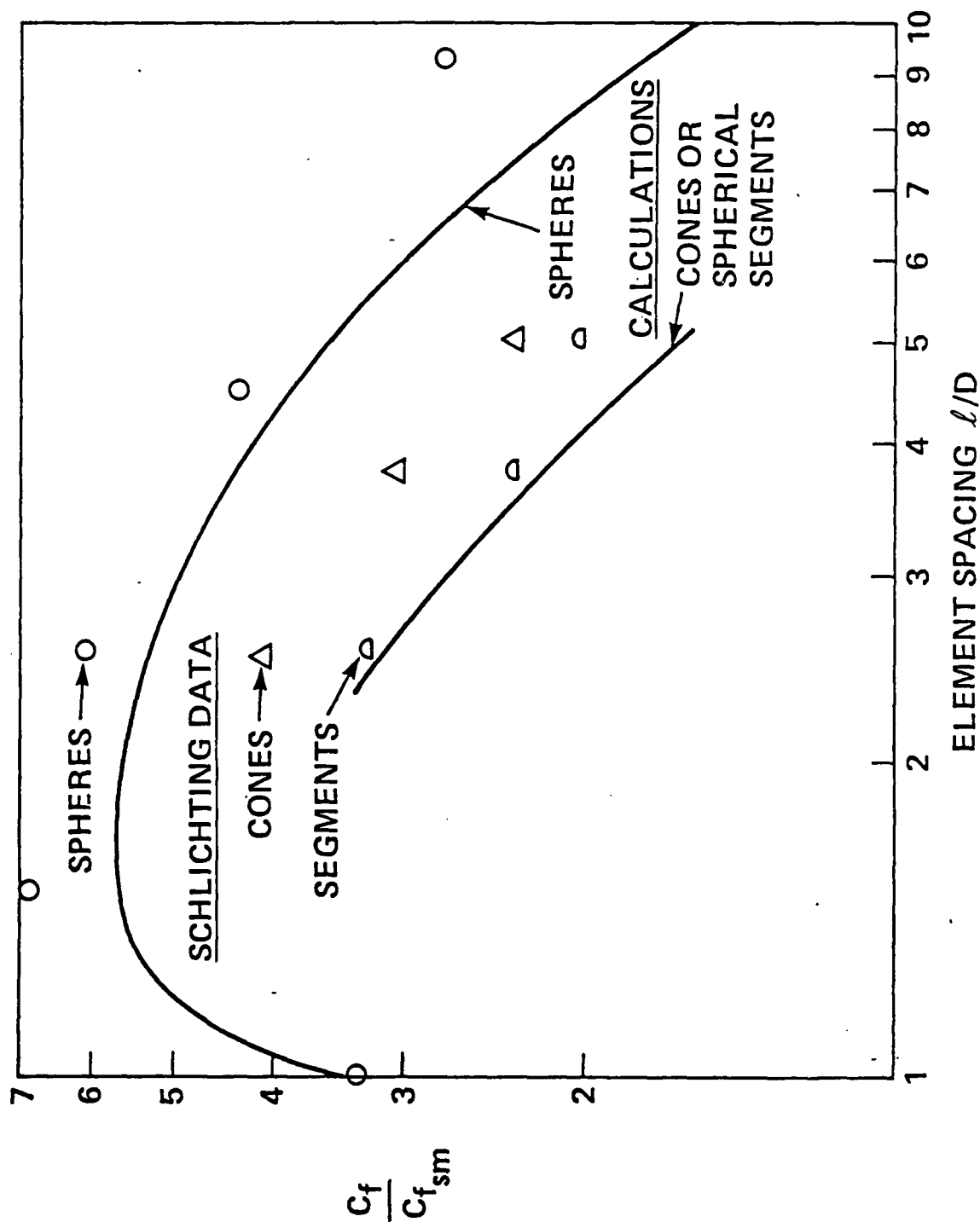friction is essentially independent of distance. The decrease in $C_f$ for spheres as $\ell/D \rightarrow 1$ is easy to explain qualitatively. At large $\ell/D$ the flow "sees" the entire sphere. With substantial element spacing, the drag increases with decreasing $\ell/D$ because there are more elements per unit area. But as $\ell/D \rightarrow 1$ the flow becomes negligible below the centers of the spheres and the drag is due only to the upper half of the elements. The cones and segments were not investigated at such close spacings. The calculations for the cones and segments are almost identical, although the cones are slightly taller, 0.375 cm vs 0.26 cm. However, the data for the cones fall above that for the segments. This implies that the effective drag coefficient for the flow about a conical roughness element is somewhat larger than that for flow about spherical elements. The same value was used in all of our calculations. If one were to allow such a higher value of $C_D$ for cones, the influence of roughness element shape would be well understood.

The second set of interesting tests was carried out by Acurex Corporation in AEDC Tunnel F,[7] using 45° conical models with a variety of surface roughnesses. This facility was an arc-driven hot shot tunnel, in which the test section pressure decreased during the run (total time $\cong$ 200 msec). The most useful tests were performed on sharp 45° cones at $M_\infty \cong 7$ at a free stream Reynolds number of $45 \times 10^6$/ft. The resulting boundary layer edge Mach number was 1.7. $N_2$ was the test gas. The first 0.75" of wetted length was roughened to 4-5 mils to ensure rapid transition.

Seven surface finishes were used on the remainder of the cone: essentially smooth, grit blasted to almost 2 mils, 2 mil bonded grit, and four chemically-etched roughness patterns (wide and close spacing at nominal heights of 4 and 10 mils). The etching process resulted in roughness elements that are best approximated as truncated cones (top radius $\cong$ 1/4 base radius) whereas the grit roughness elements are simulated with hemispheres. The roughness characteristics of these chemically milled surfaces varied by as much as ± 30% in mean roughness height over the surface of the cones. Table I lists the average element height and spacing for the various surfaces. Note that the "4 mil" etched roughness is actually considerably less rough. Also, the "4 mil" roughnesses have larger relative roughness spacing than the "10

TABLE I.    Roughness Characteristics for Acurex AEDC Tests at Mach 7

| Designation | Mean k (mils) | Mean Spacing $\ell$ (mils) | $\rho_e u_e \left( \dfrac{kg}{m^2 sec} \right)$ |
|---|---|---|---|
| Smooth | --- | --- | 2038 |
| Grit Blasted | 1.63 | 7.70 | 2235 |
| Bonded Grit | 2.00 | 4.00 | 2292 |
| 4 mil Wide | 3.00 | 23.0 | 2157 |
| 4 mil Close | 2.50 | 13.0 | 2357 |
| 10 mil Wide | 10.32 | 56.0 | 1998 |
| 10 mil Close | 9.50 | 31.0 | 2315 |

mil" surfaces. In fact, the "4 mil close" and "10 mil wide" roughnesses have essentially the same $\ell/k$.

The primary measurements for this test series are the heat transfer rates, determined by thin wall calorimetry with thermocouples on the back wall. Some co-axial heat transfer gauges, as well as skin friction gauges, were also used, although there may be uncertainties regarding how faithfully the roughness is reproduced on the surface of the gauges. The skin friction measurements are limited and show such scatter that few conclusions are possible (see Ref. 8 for more discussion).

Figure 5 compares the Stanton numbers, $q/\rho_e u_e C_p (T_r - T_w)$, calculated by the present model with the Acurex data.[7]* The agreement is seen to be good, with the theory generally well within the scatter of the data. Several trends are evident from either data or calculations. The bonded grit and grit blasted surfaces cause a similar heating augmentation, although the bonded grit is slightly taller and considerably more densely packed; a blockage effect must be counter-acting the more obvious effect of element spacing. However, for the chemically etched surfaces, spacing appears to be more important than height. The 10-mil wide spacing yields a greater heating rate than the 4-mil (actually 3-mil) wide case only at larger distances, and the 4-mil and 10-mil close spacing results are also quite similar. As already noted, the relative roughness spacing is not constant between the 4- and 10-mil heights, and a more detailed discussion of the dependence of height, shape and spacing is presented below.

Another interesting experiment on roughness effects has been conducted in the hypersonic shock tunnel at Calspan.[9] Only one roughness was studied — a bonded grit similar to that employed by Acurex in the series discussed above. The mean roughness height was 3.8 mils, with a spacing of 10-15 mils (we specified 12.5 mils for the spacing). As with the Acurex

---

*The data points have actually been derived by dividing the reported heat transfer coefficients by our computed values of $\rho_e u_e$ and the specific heat of $N_2$. Table I includes the values used for $\rho_e u_e$ for the various cases. Note that $\rho_e u_e$ varies by as much as 18% from one case to another, and examination of the heat transfer rate (q) rather than the Stanton number could possibly lead to inaccurate conclusions on the effect of roughness.
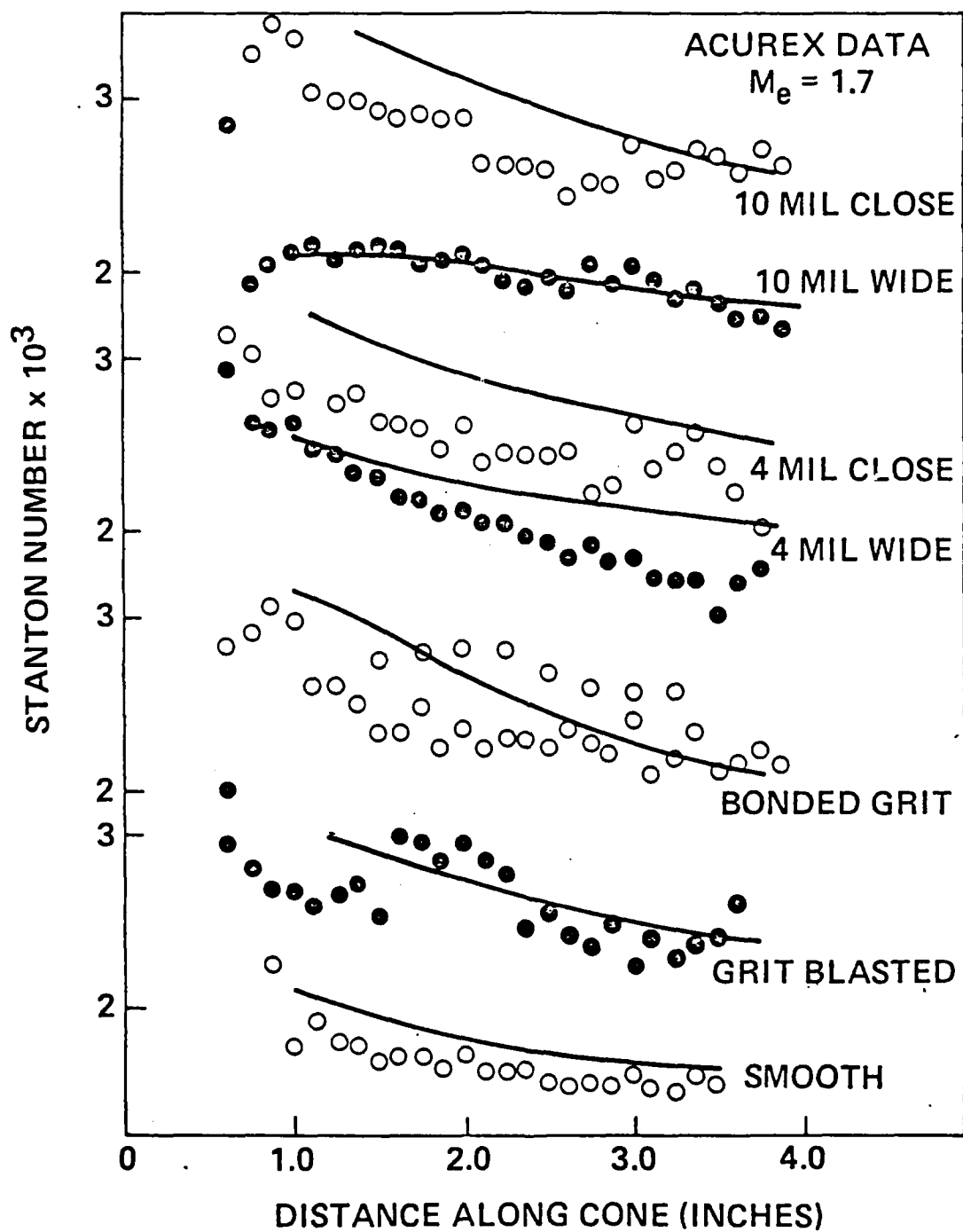
Fig. 5 Heat transfer coefficient comparisons for various
surface roughnesses — 45° cones at $M_\infty = 7$.

series, the models were 45° cones. The free stream Mach number was 11-13, although this larger value has little effect on the edge Mach number, due to the large cone angle. $T_w/T_e$ is considerably less in the Calspan conditions. Heat transfer was measured with thin film gauges covered with the surface roughness. Figure 6 shows our comparison with Holden's results, for smooth and roughened surfaces, on a sharp 45° cone at the highest Reynolds number tested. The smooth wall boundary layer was naturally turbulent near the nose. It is evident that the model yields heating rates about 15% higher than measured, even for the smooth wall. The measured smooth wall Stanton number is consistent with values predicted from accepted engineering methods such as that of van Driest[10] (St $\cong$ 2.56 x $10^{-3}$). The reason for this discrepancy is not clear, although it may be associated with numerical inaccuracies that arise with large density differences across the boundary layer. In any case, the present model predicts a degree of roughness heating augmentation comparable to that observed.

The first high Mach number tests with distributed surface roughness were conducted by Keel[11] on 5° sharp cones in Tunnel No. 2 at the Naval Surface Weapons Center, at $M_\infty$ = 5 or $M_e$ = 4.77. Sand grains were uniformly applied to the model with epoxy, yielding roughness heights of either 23 mils or 43 mils. Element spacing measurements were not reported, and we assumed a value ($\ell/D$ = 2.5) which is typical of the bonded grit surfaces constructed by Acurex[7] and Calspan.[9] Skin friction and heat transfer were measured with floating element balances and slug calorimeter gauges, respectively.

One noteworthy aspect of Keel's experiment is that the measurements were obtained at a fixed station on the cone, x = 2 ft. The Reynolds number was varied by decreasing the tunnel pressure, and the results plotted as $C_f$ or St vs $Re_\theta$ (see Fig. 7). The manner by which the data were collected must be recognized to properly interpret these results. With a smooth wall, $C_f$ is a function only of $Re_\theta$ (assuming fixed values of $M_e$ and $T_w/T_e$) and one may equally well traverse the $C_f$ vs $Re_\theta$ curve by varying pressure (i.e., density) or distance (i.e., $\theta$). However, a second independent parameter enters with rough walls. For simplicity, let us use
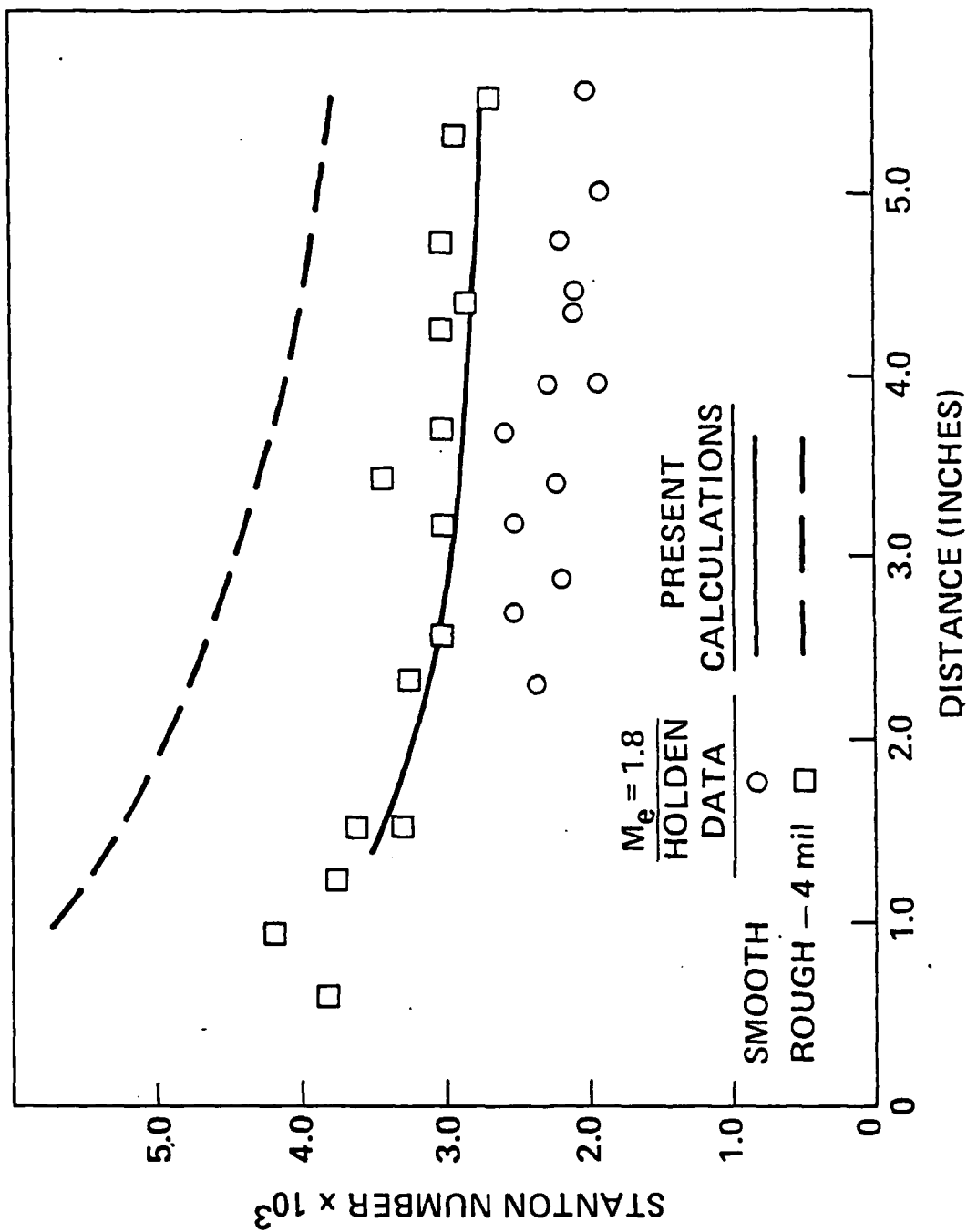
$$k^+ = \rho_w u_\tau k/\mu_w$$

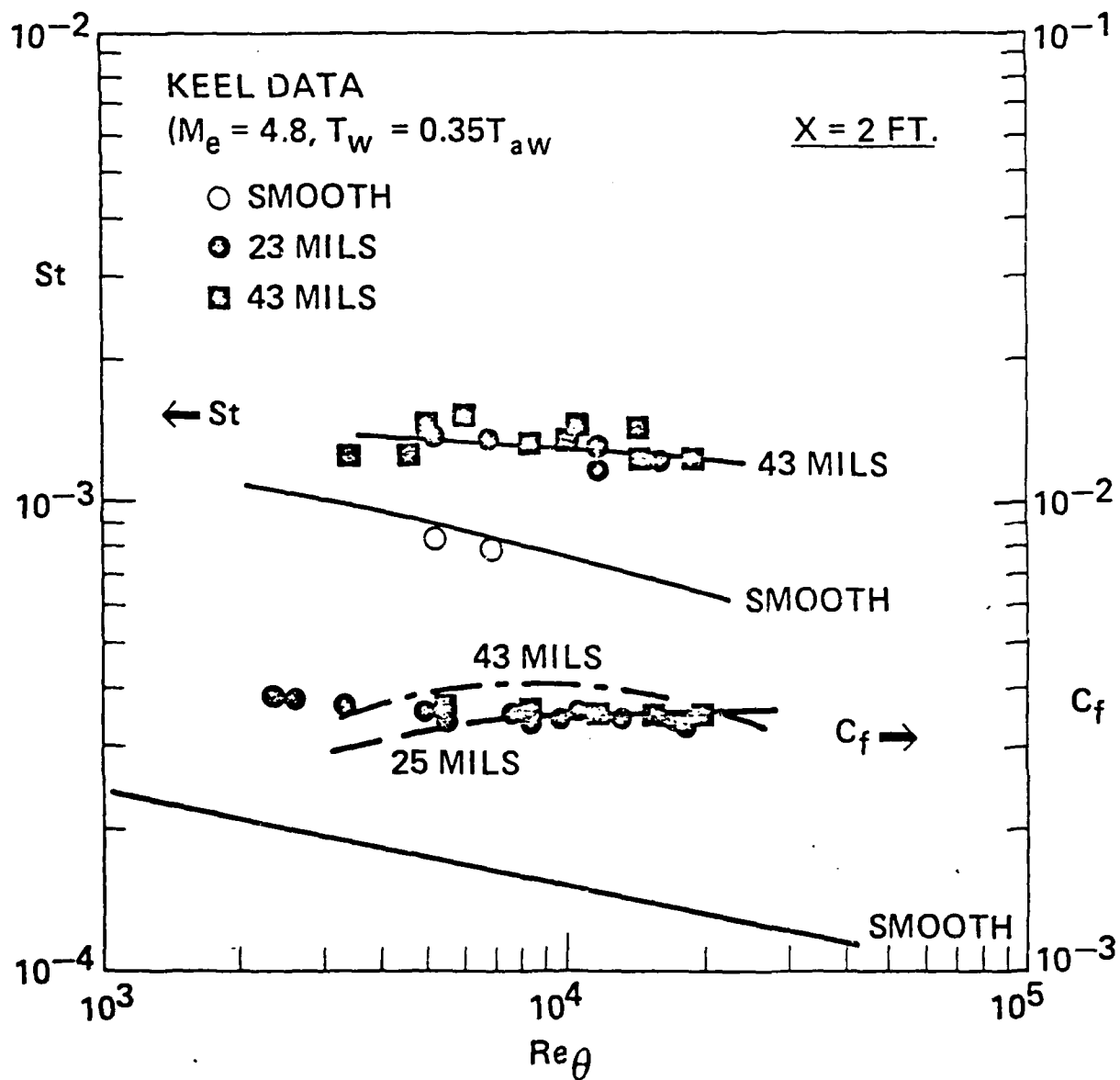Fig. 6  Comparison of present theory with Holden's data for smooth and rough (4 mil bonded grit).

Fig. 7 Comparison of present theory with Keel's heat transfer and skin friction data — $M_e = 4.8$, $k = 23$ and 43 mils.

as the fundamental parameter to describe the roughness augmentation effect. Furthermore, $u_\tau/u_e$ is a very weak function of $Re_\theta$ and may be considered constant for the purposes of this argument. Thus, if we consider increasing distance along a flat plate or cone, $Re_\theta$ increases because $\theta \sim x^{0.8}$, while $k^+$ remains constant. Conversely, when Keel raises the pressure at a fixed station, both $Re_\theta$ and $k^+$ increase together, linearly with the density. This offers an explanation for the almost complete absence of slope for the data in Fig. 7; the increasing roughness augmentation (with increasing $k^+$) tends to cancel the natural tendency of $C_f$ or St to decrease with increasing $Re_\theta$. Agreement with the data is very good - $k^+$ is apparently sufficiently large that the roughness augmentation is nearly saturated and there is little difference between 23 and 43 mils. It should be noted that the computed Mach number at the tops of the elements is barely supersonic in this case.

For hypersonic edge conditions, Fig. 8 shows a comparison with the heat transfer data obtained by Hill[12] at NSWC on a 7° sharp cone at $M_e = 8$ and $Re_\infty = 7 \times 10^6$/ft. The roughness heights are based on the nominal sizes of the grits that were applied to the surface. We simulated the roughness with hemispheres of height equal to the nominal values, with a spacing of 2.9k, as indicated by surface profilometer measurements. It is evident from Fig. 8 that the computer model yields approximately the observed heat transfer augmentation as a function of roughness height, although the data show less dependence on distance. The reasons for this discrepancy are not clear.

An even more intriguing set of hypersonic data have been obtained by Holden[13] in the Calspan shock tunnel. In this case the edge Mach number is 9.4, the cone half-angle is 6°, and the free-stream Reynolds number for the cases of interest is $1.1 \times 10^7$/ft. Again, we simulated the roughness with hemispheres with height equal to the nominal grit sizes. In this case, however, the elements are rather tightly packed, $\ell/k \cong 2.25$. Figure 9 shows that the theory yields a trend of increasing heat transfer with increasing roughness, while the data show significant decreases. There are several possible explanations for the observed reductions in heat transfer. One
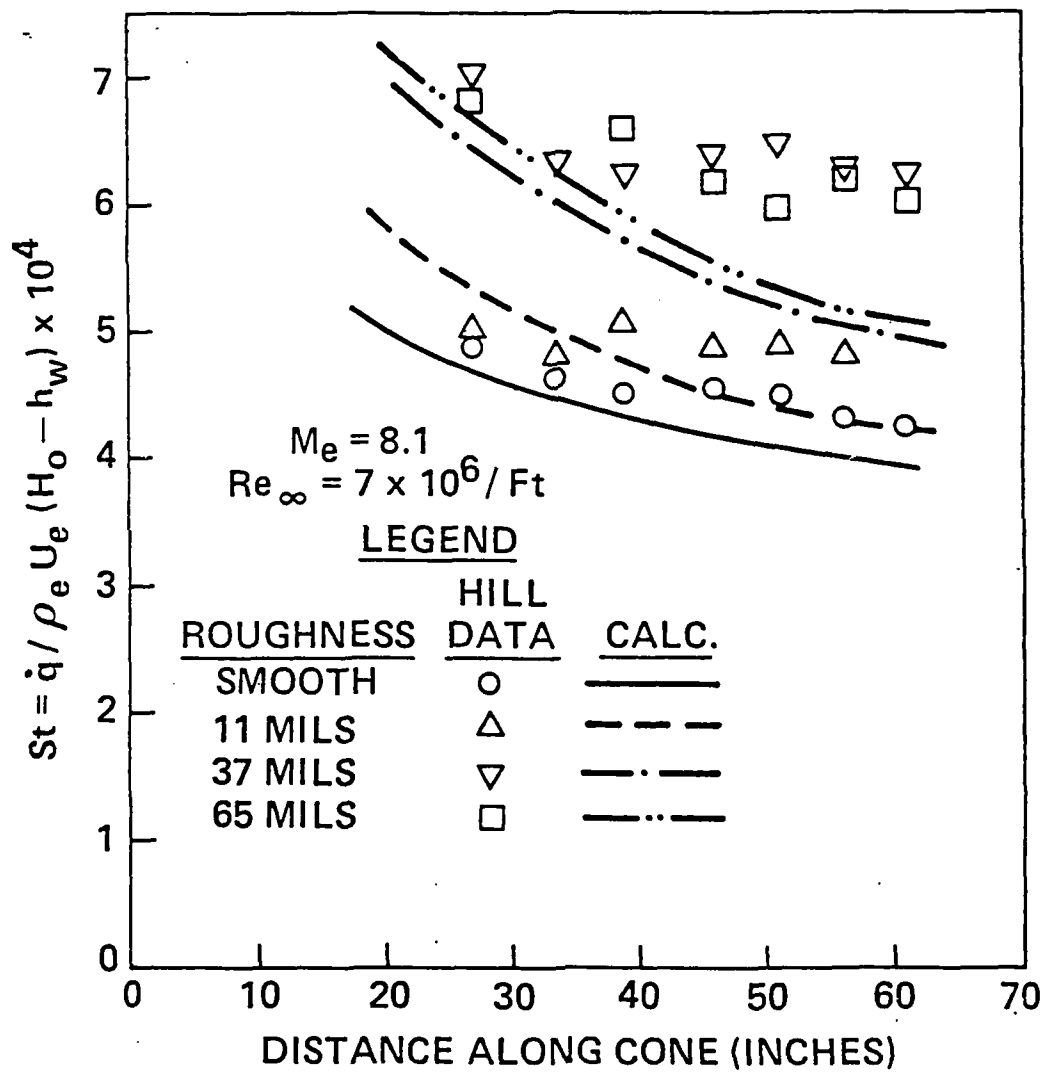
Fig. 8  Comparison of present theory with Hill's data for smooth and rough surfaces at an edge Mach number of 8.
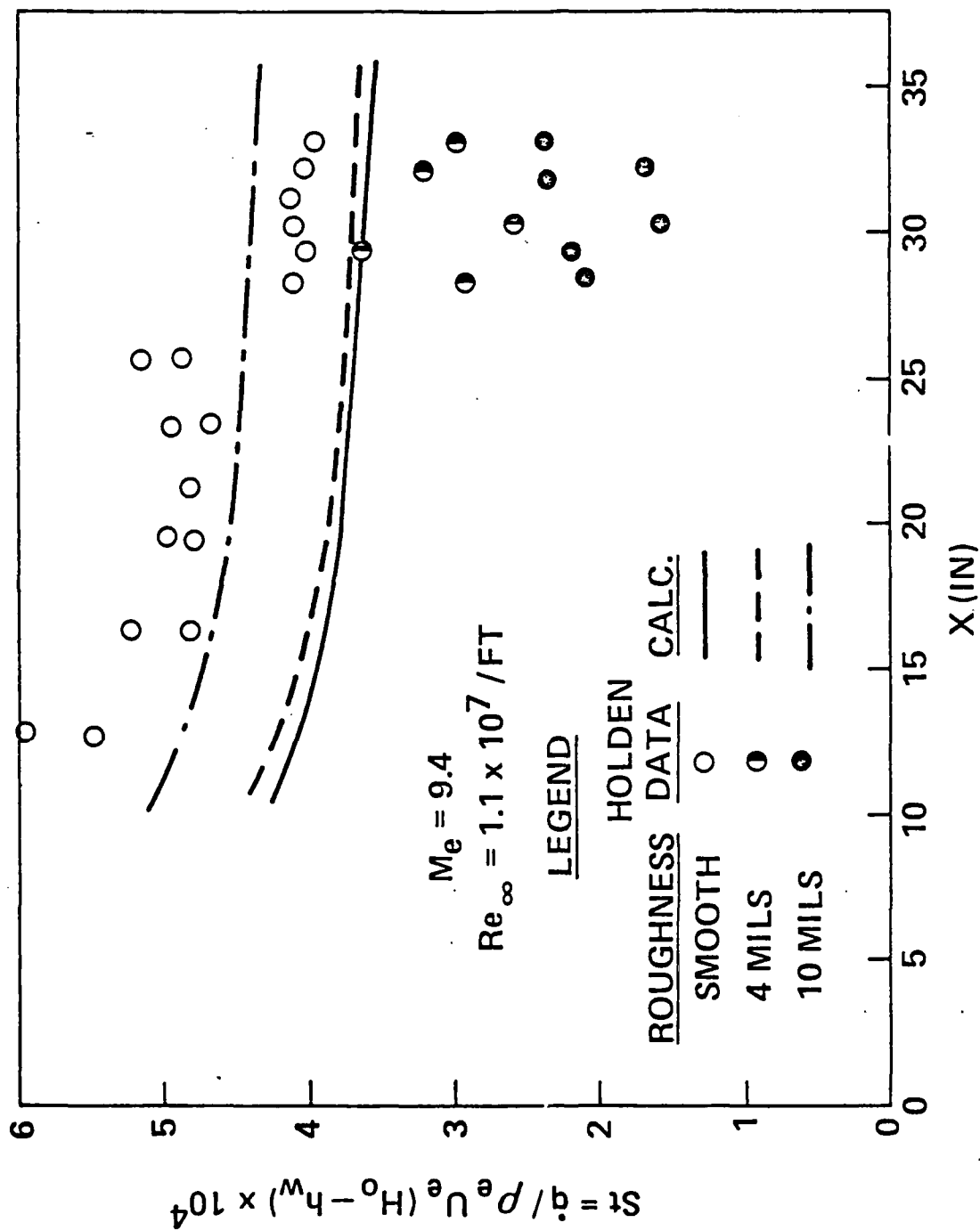
Fig. 9  Comparison of present theory with Holden's data for smooth and rough
surfaces at an edge Mach number of 9.4.

is associated with the tight packing of the elements. However, our calcu-
lations show that there might be a modest reduction in the heating augmen-
tation as $\ell/D \to 1$ (cf. Fig. 4), but not below smooth wall values. Further-
more, Holden's data on 45° cones at $M_e = 1.8$, with a similar 4 mil bonded
grit roughness, were presented above in Fig. 6 and showed no reduction
below smooth wall values. A second possibility has to do with upstream
behavior; the rough wall boundary layer may simply be much thicker at a
given station. Again, the present calculations do not indicate any such
reversal effect. A third possibility has to do with the high Mach number,
which could result in locally supersonic flow, shock waves around the ele-
ments, and perhaps an alteration of the drag or heating laws. In fact,
Holden's[13] shadowgraph observations indicate a significant wave structure
emanating from the rough surface. But, our computed local Mach numbers
are only barely supersonic (1.14) at the tops of the elements, no more
supersonic than in the Keel case discussed above. A related Mach number
effect, discussed in more detail below, is that roughness causes increased
boundary layer temperatures at high edge Mach numbers; perhaps more careful
calculations would show a reduction below smooth wall values. In any case,
the matter is not resolved, particularly in light of the similar conditions
of the experiments of Hill and Holden. Clearly, more measurements and
calculations are needed.

## IV. ROUGHNESS SCALING BEHAVIOR

A major advantage of the present type of numerical study is that the solutions can be scrutinized to determine the nature of roughness effects. Of course, the data comparisons shown in the previous section left several issues unresolved, but, nevertheless, a detailed examination of the numerical results is justified. The results are quite interesting.

The most striking aspect of our solutions is that the mean velocity is computed to be quite uniform over much of the range y < k. A typical example is shown in Fig. 10. Of course, very near the wall (i.e., at the bottom of the elements) the velocity must be zero, and near the tops of the elements the velocity tends to increase. This constant velocity, which was unexpected, is evident in almost all of the cases considered, the sole exceptions being cases with very small roughness (say $k^+ \leq 10$) or very large roughness ($k/\theta > 1$). Within the range of constant velocity, production of turbulent energy is negligible; the turbulence simply diffuses toward the wall and dissipates. In the mean velocity equation (Eq. 3) only the final two terms, representing turbulent shear and form drag on the elements, are important. The total drag on the elements, which should be close to the actual rough wall skin friction, is easily related to the element shape and spacing

$$C_f \sim f(y) \int_0^k \frac{\rho U^2}{\rho_e U_e^2} \, C_D \, \frac{D(y)dy}{\ell^2} \cong f(y) \, \frac{\rho_R U_R^2}{\rho_e U_e^2} \, C_D \int_0^k \frac{D(y)dy}{\ell^2} \, . \tag{6}$$

Here we use $(\ )_R$ to denote conditions in the region of constant velocity.

The integral in Eq. 6 is the frontal area of the elements per unit superficial surface area. This quantity is easily related to the shape and density of roughness elements. However, to compute the skin friction the roughness velocity $U_R$ is also needed (determination of $\rho_R$, as well as the relation between heat transfer and skin friction, will be addressed below).

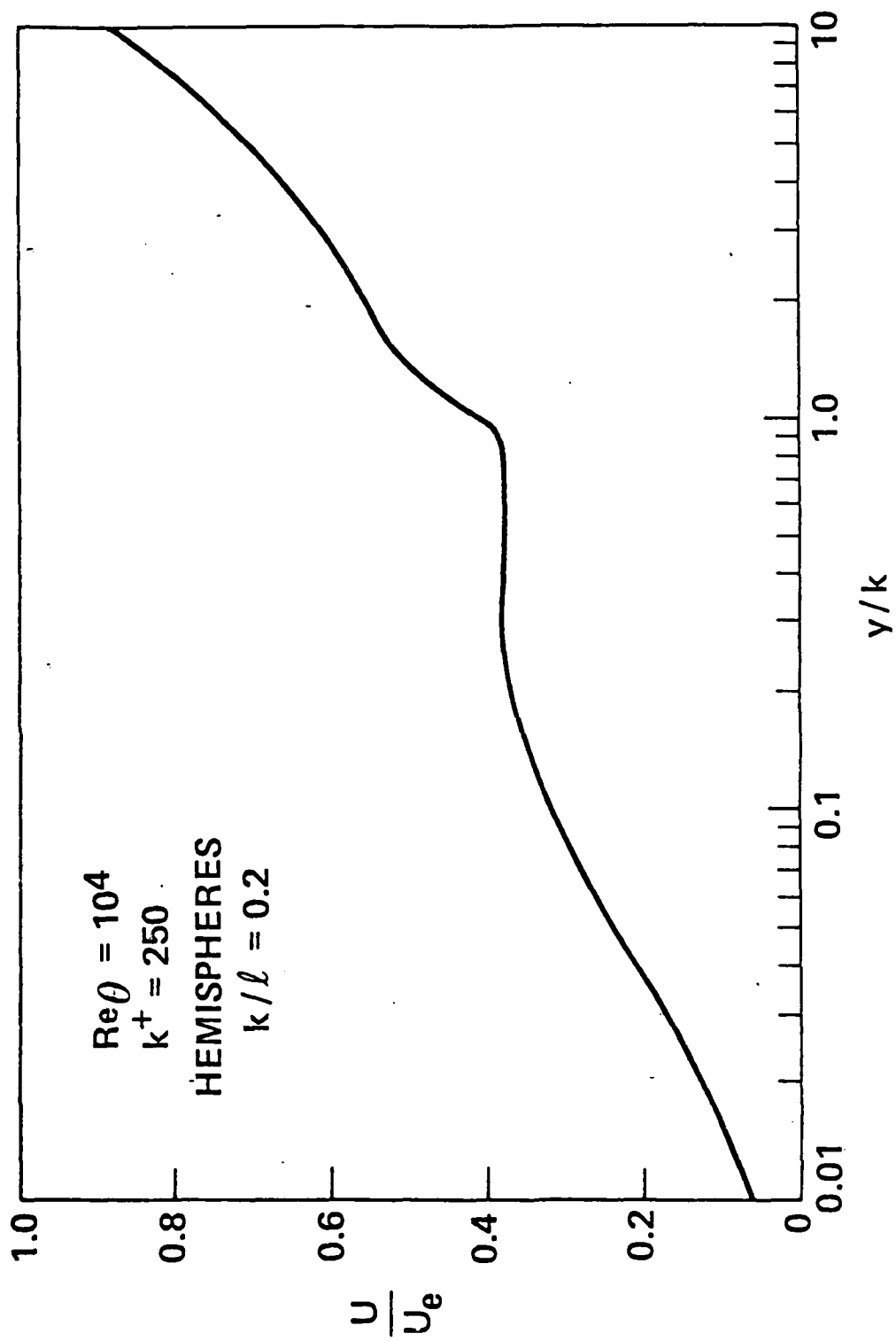Fig. 10  Calculated mean velocity profile for a typical rough wall case.

The plot shows $U/U_e$ on the vertical axis (from 0 to 1.0) versus $y/k$ on the horizontal axis (logarithmic scale from 0.01 to 10).

$Re_\theta = 10^4$
$k^+ = 250$
HEMISPHERES
$k/\ell = 0.2$

We have been unable to predict $U_R$ by any simple theoretical arguments. Accordingly, the computer model was systematically run over a range of parameters, including element shape, spacing, height, $T_W/T_e$, and $M_e$. To be specific, $U_R$ was defined to be the mean velocity at $y = k/2$.

Figure 11 shows the computed roughness velocity for hemispheres in incompressible conditions. The roughness spacing varies along the abscissa; $U_R$ is normalized by the smooth wall velocity at $y = k/2$ (easily computed from the classic law-of-the-wall). Only a slight dependence on $Re_\theta$ is apparent. It should be emphasized that only roughness spacing and downstream distance ($Re_\theta$) were varied to obtain these curves. However, the really significant finding is that the same curves apply to variations in element shape, height, $T_W/T_e$, and $M_e$. In addition to hemispheres, we also considered 30° conical elements (base diam = k), 45° cones (base diam = 2k), truncated 30° cones (base diam = k, top diam = k/2), and cylinders (base diam = k). For each of these shapes the results were indistinguishable from those of Fig. 11. There is a dependence on roughness height ($k^+$), as illustrated in Fig. 12, but the trend is slight unless $k^+$ is less than about 20 (as $k^+ \to 0$, $U_R/U_S \to 1$, but the smooth wall shear would dominate anyway). Varying the wall temperature over the range $T_W/T_e = 0.2 - 1.0$ has little effect, as does increasing the edge Mach number up to at least 8.

The substantial effect of roughness on the velocity profile is not observed with the enthalpy profile. This undoubtedly results from the fact that there is no heat transfer mechanism analogous to form drag. In Fig. 13 we compare normalized total enthalpy values at $y = k/2$ with the roughness velocity. At $M_e = 0$, the rough and smooth wall enthalpies at $y = k/2$ are identical within the accuracy of our computations, even for large temperature differences across the boundary layer ($T_W = T_e/5$). At supersonic velocities, the total enthalpy is obviously reduced by smaller margins than is the velocity. There appears to be a hypersonic limit, with $\tilde{H}_R/\tilde{H}_S \sim (U_R/U_S)^{1/2}$, although more computations would be required to confirm this.

- 24 -

Fig. 11 Ratio of computed roughness velocity (y = k/2) to smooth wall velocity at the same height, as a function of projected roughness element area and $Re_\theta$.
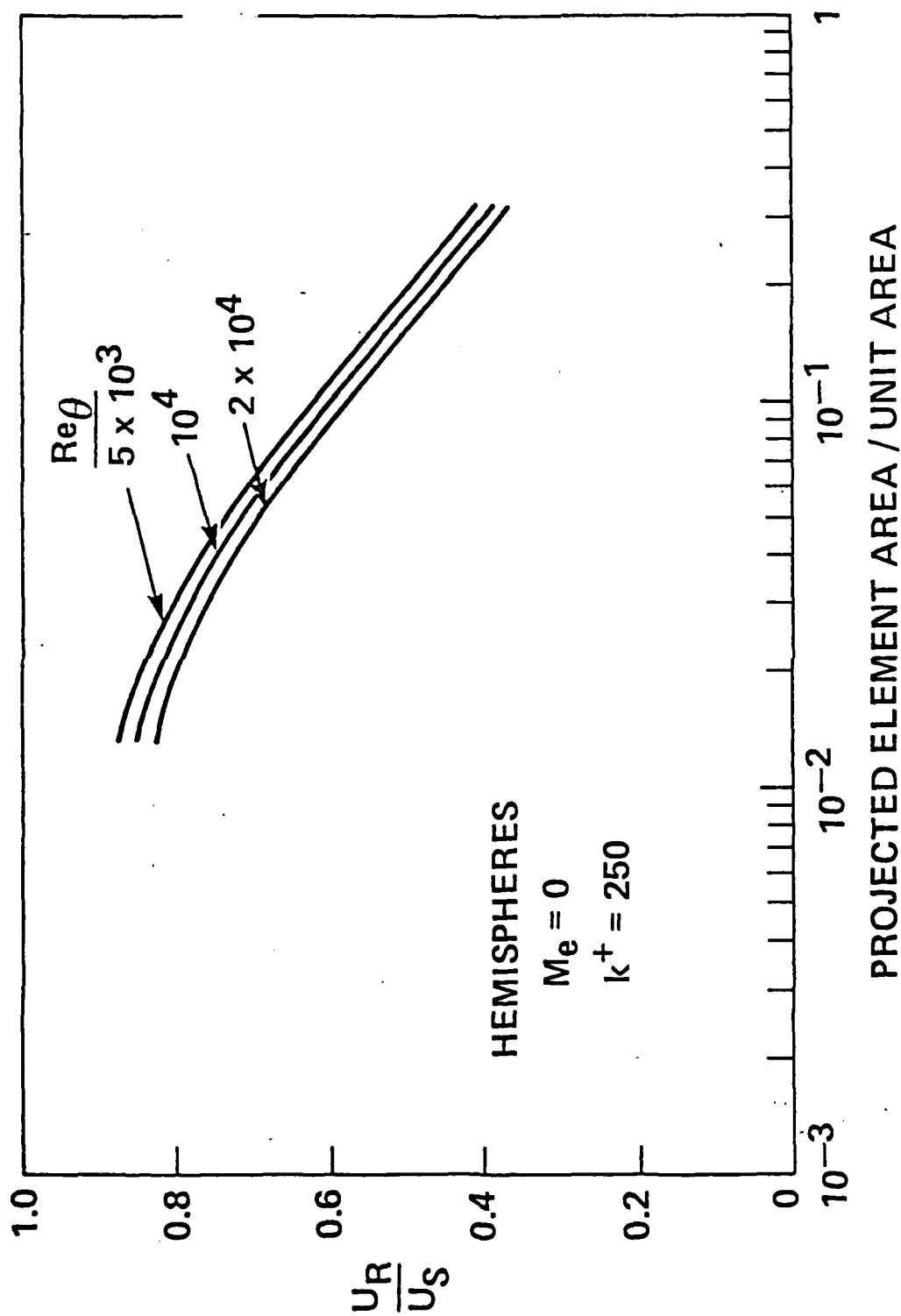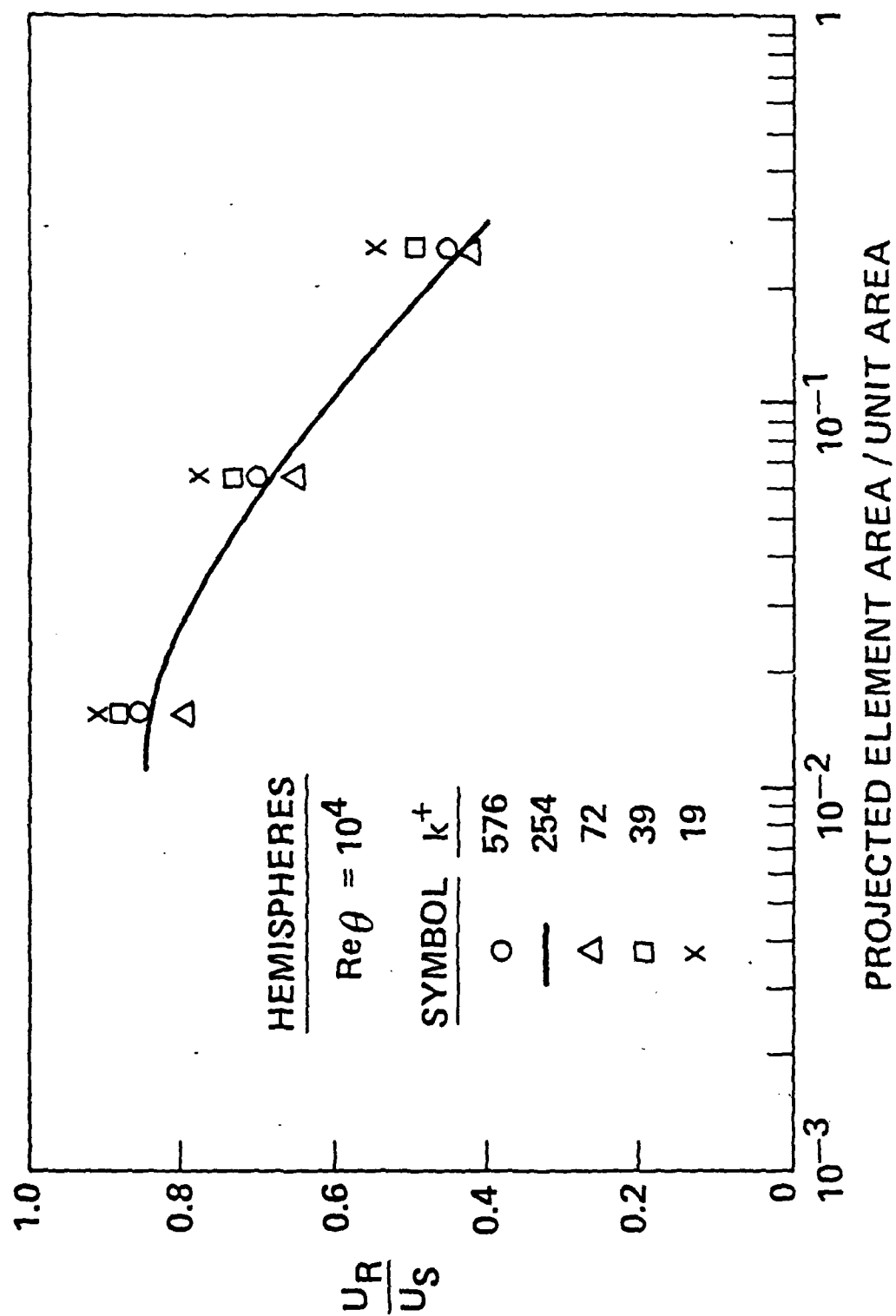
Fig. 12  Ratio of computed roughness velocity (y = k/2) to smooth wall velocity at the same height, as a function of projected roughness element area and $k^+$.
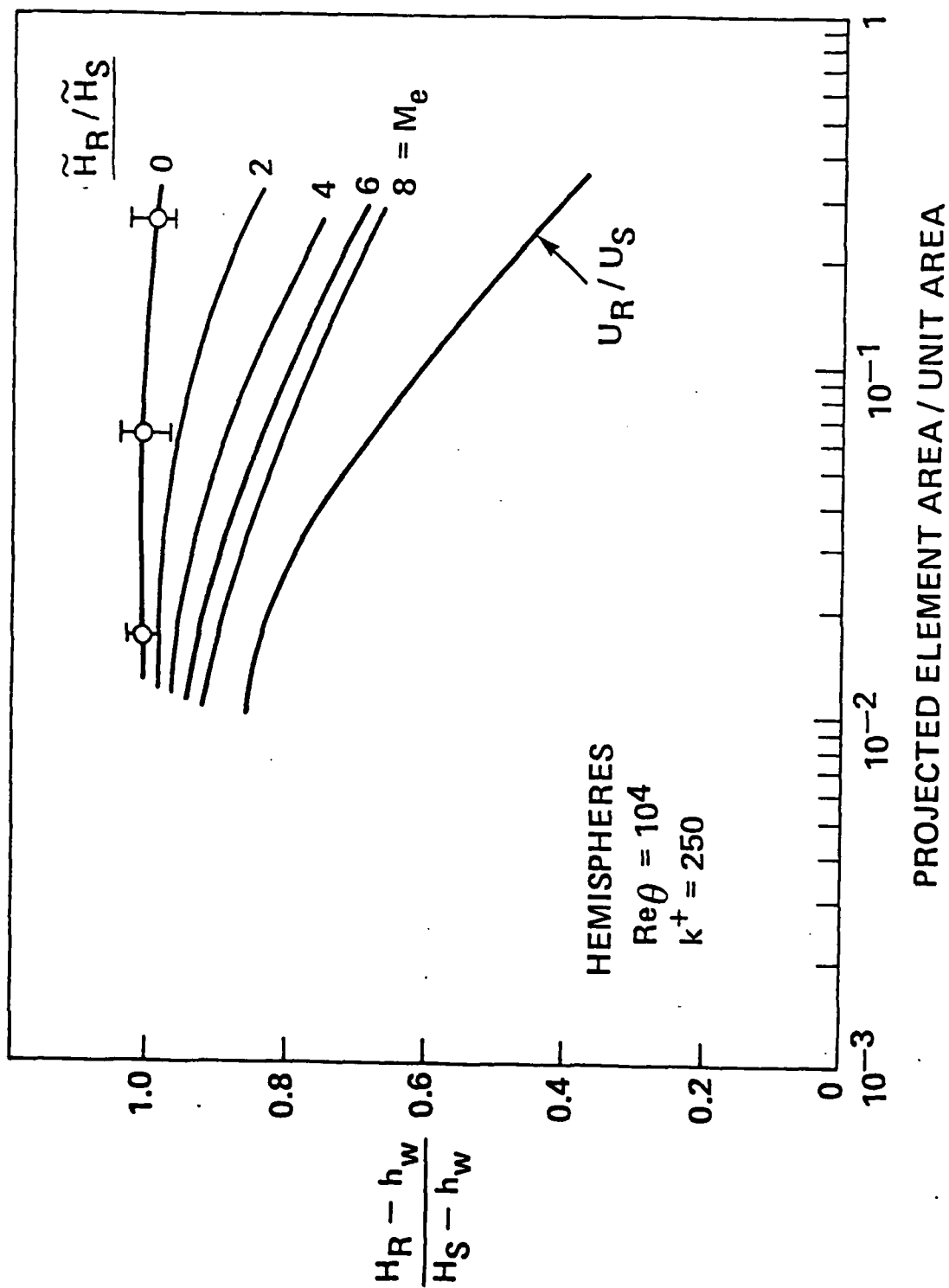
Fig. 13 Ratio of computed total enthalpy $(y = k/2)$ to smooth wall enthalpy at the same height, as a function of projected element area and edge Mach number.

An important consequence of Fig. 13 is that roughness will tend to increase the static enthalpy for y<k at supersonic velocities. The resulting decrease in density will reduce the form drag on the elements, and the increased temperature will reduce the underlying smooth wall skin friction. Thus our calculations suggest a specific Mach number dependence for roughness friction or heating augmentation. The compensating effect of increased temperatures reduces roughness augmentation at high Mach numbers; if this is somewhat greater than we have estimated, it could offer an explanation for the decreases in heat transfer observed by Holden.

Finally, we might note two additional trends that are well established by our numerical results. First, the underlying smooth wall skin friction is, to a good approximation, unchanged by roughness (fixed value of $Re_\theta$), except for the high Mach number effect just mentioned. Secondly, the increase in heat transfer is nicely described by the square root of the skin friction augmentation. The reason was given in our previous study[5]: roughness increases fluctuating velocities but not fluctuating temperatures, and the turbulent stress goes as $-\rho\overline{u'v'}$ while the turbulent heat flux goes as $-\rho\overline{u'T'}$.

## V. ROUGHNESS SCALING FORMULAE

It is useful to summarize the relations needed to predict roughness effects on skin friction and heat transfer, particularly since the present results are in a very different form from existing methods. First, the skin friction and heat transfer augmentations are given by

$$C_f = C_{f_S} + \frac{\rho_R U_R^2}{\rho_e U_e^2} C_D \int_0^k \frac{D(y)dy}{\ell^2} \; f(k/2) \quad , \tag{7}$$

$$\frac{St}{St_S} = \left( \frac{C_f}{C_{f_S}} \right)^{1/2} . \tag{8}$$

The smooth wall values may be obtained from a variety of well-known sources, such as Ref. 10. The integral in Eq. (7) requires the roughness element shape and spacing, and $f(k/2)$ follows from Eq. (4). We recommend $C_D = 0.6$. The ratio $U_R/U_S$ may be obtained from Figs. 11 or 12, and the smooth wall velocity at $y = k/2$ from the standard law-of-the-wall:

$$\frac{U_S}{U_{\tau_S}} = 2.5 \, \ell n \left( \frac{U_\tau y}{\nu_w} \right) + 5 \;, \quad \frac{U_{\tau_S}}{U_e} \sqrt{\frac{\rho_e}{\rho_w} \frac{C_{f_S}}{2}} . \tag{9}$$

The roughness density appearing in Eq. (7) requires slightly more algebra. Assuming a perfect gas,

$$\left( \frac{\rho_R}{\rho_S} \right)^{-1} = \frac{h_R}{h_S} = \left( 1 + \frac{\gamma-1}{2} M_S^2 \right) \frac{H_R}{H_S} - \frac{\gamma-1}{2} M_S^2 \frac{U_R^2}{U_S^2} \;, \tag{10}$$

$$M_S = M_e \frac{U_S}{U_e} \left( \frac{h_S}{h_e} \right)^{-1/2} . \tag{11}$$

It is adequate to use a Reynolds analogy for the smooth wall total enthalpy, $(H - h_w)/(H_0 - h_w) = U/U_e$, to estimate the smooth wall static enthalpy:

$$\frac{h_S}{h_e} = \frac{h_w}{h_e} + \left(1 + \frac{\gamma-1}{2} M_e^2 - \frac{h_w}{h_e}\right) \frac{U_S}{U_e} - \frac{\gamma-1}{2} M_e^2 \frac{U_S^2}{U_e^2} \ . \tag{12}$$

And, the total enthalpy ratio in Eq. (10) is directly related to the normalized total enthalpy difference

$$\frac{H_R}{H_S} = \frac{h_w/h_S + \left(1 + \frac{\gamma-1}{2} M_S^2 - h_w/h_S\right)\frac{\tilde{H}_R}{\tilde{H}_S}}{1 + \frac{\gamma-1}{2} M_S^2} \ . \tag{13}$$

Taking $\tilde{H}_R/\tilde{H}_S$ from Fig. 13, Eqs. (10)-(13) are sufficient to provide $\rho_R/\rho_e$.

Finally, at high Mach numbers, the temperature increase due to roughness can reduce the smooth wall friction coefficient or Stanton number. To estimate this effect, we suggest modifying a simple reference enthalpy method. The smooth wall coefficients are inversely proportional to the reference enthalpy, which in turn depends on the peak boundary layer enthalpy

$$\frac{h_{ref}}{h_e} \cong 1 + 0.7 \left(\frac{h_{peak}}{h_e} - 1\right) \ . \tag{14}$$

For a smooth wall, $h_{peak}$ may be estimated by taking the maximum of Eq. (12) with respect to $U_S$:

$$\frac{h_{peak,S}}{h_e} = \frac{h_w}{h_e} + \frac{\left(1 + \frac{\gamma-1}{2} M_e^2 - \frac{h_w}{h_e}\right)^2}{4 \frac{\gamma-1}{2} M_e^2} \ . \tag{15}$$

However, if the rough wall enthalpy resulting from Eq. (10) is greater tan the value obtained from Eq. (15), then the smooth wall friction coefficient and Stanton number should be reduced by the factor

$$\frac{1 + 0.7 \left( \dfrac{h_{peak,S}}{h_e} - 1 \right)}{1 + 0.7 \left( \dfrac{h_R}{h_e} - 1 \right)} \qquad . \qquad (16)$$

# VI.  DISCUSSION

The present rough wall Reynolds stress model yields results that compare acceptably with a variety of available measurements.  Of the several discrepancies noted, the most significant is that with Holden's high Mach number tests.  The matter may not be resolved until additional high Mach number data are obtained.  The observed decrease in heating rates could be due to the extreme close packing of the roughness elements, although our model fails to confirm this.  The model does suggest that the increased temperatures generated by roughness at high edge Mach numbers tend to reduce skin friction and heat transfer.  However, these findings are only suggestive, and one cannot at this time rule out an experimental artifact or a significant change in the nature of flow about roughness elements in supersonic conditions.

The roughness scaling behavior derived from our systematic variation of the several relevant parameters suggests scaling laws that are a major departure from previous approaches.  The influence of roughness element shape and spacing is almost totally defined by the projected frontal area per unit surface area.  The velocity that gives rise to form drag is largely constant over the $y \leq k$.  When normalized by the smooth wall velocity at $y = k/2$, this roughness velocity is primarily a function of this projected element area/unit area.

A simple method is thus provided for predicting and analyzing roughness character effects.  However, it must be admitted that the relations given here need additional evaluation and refinement before they can be used with great confidence.  For example, the minor dependence of $U_R/U_S$ on $k^+$ and $Re_\theta$ should be better defined by additional calculations, and much more hypersonic data ought to be studied to substantiate the Mach number dependence.

## RESEARCH STAFFING AND PUBLICATIONS

Dr. Michael L. Finson was the Principal Investigator. Dr. Finson was assisted by Mr. A. S. Clarke, Dr. H. H. Legner and Dr. P. K. S. Wu.

Results of this work was presented as AIAA Paper P80-1459 (which is essentially identical to this report) and have also been submitted to Program Series in Astronautics and Aeronautics.

The personnel involved in this program have maintained contact and provided consulting to various programs supported by the Air Force Ballistic Missile Office, as well as related experimental programs supported by Air Force Office of Scientific Research.

REFERENCES

1.  Nikuradse, J., "Strömungsgesetze in rauhen Rohren," VDI Forschung-
    sheft, No. 361, SerB, Vol. 4, (1933); English Translation, NACA
    TM1292, 1950.

2.  Schlichting, H., "Experimental Investigation of the Problem of
    Surface Roughness," NACA TM823 (1937). Also Bounday Layer Theory,
    McGraw-Hill, New York (1968).

3.  Bettermann, D., "Contribution a l'Etude de la Connection Forces
    Turbulente le Long de Plaques Rugueuses," Int. J. Heat & Mass Trans-
    fer 9, 153-164 (1966).

4.  Dvorak, F. A., "Calculation of Turbulent Boundary Layers on Rough
    Surfaces in Pressure Gradient," AIAA Journal, Vol. 7, No. 9, Sept.
    1969, pp. 1752-1759. Also AIAA J., Vol. 4, No. 11, Nov. 1972,
    pp. 1447-1451.

5.  Finson, M. L. and Wu, P. K. S., "Aanalysis of Rough Wall Turbulent
    Heating with Application to Blunted Flight Vehicles," AIAA Paper
    79-008 (1979). Also PSI TR-158, AFOSR-TR-79-0199.

6.  Saffman, P. G. and Wilcox, D. C., "Turbulence-Model Predictions
    for Turbulent Boundary Layers," AIAA Journal, Vol. 12, No. 4, April
    1974, pp. 541-546.

7.  Foster, T., Read, D., and Murray, A., "Reduced Data Report: Sur-
    face Roughness Heating Augmentation Tests in AEDC Tunnel F., Vol.
    II," Acurex Report TR-79-183 (1979).

8.  Finson, M. L., Clarke, A. S., and Wu, P. K. S., "Effect of Surface
    Roughness Character on Turbulent Boundary Layer Heating," PSI TR-
    204 (1979).

9.  Holden, M. S., "Studies of the Effects of Transitional and Turbulent
    Boundary Layers on the Aerodynamic Performance of Hypersonic Re-
    entry Vehicles in High Reynolds Number Flows," Calspan Rep. AB-
    5834-A-2, AFOSR-TR-79-0125, (1978).

10. Hopkins, E. J., and Inouye, M., "An Evaluation of Theories for
    Predicting Turbulent Skin Friction and Heat Transfer on Flat Plates
    at Supersonic and Hypersonic Mach Numbers," AIAA Journal, Vol. 9,
    No. 6, June 1971, pp. 993-1003.

11. Keel, A. G., Jr., "Influence of Surface Roughness on Skin Friction
    and Heat Transfer for Compressible Turbulent Boundary Layers,"
    AIAA Paper 77-178, (1977).

REFERENCES (Cont.)

12.    Hill, J. A. F., "Measurements of Surface Roughness Effects in the Heat Transfer to Slender Cones at Mach 10," AIAA P-80-0345 (1980).

13.    Holden, M. S., "Accurate Vehicle Experimental Dynamics Program. Final Report. Studies of Aero-Thermodynamic Phenomena Influencing the Performance of Hypersonic Re-entry Vehicles," Calspan Corporation. SAMSO-TR-79-47 (1979).

## APPENDIX

## REYNOLDS STRESS MODEL EQUATIONS

The governing partial differential equations for the various turbulent quantities are listed here. For more details, the reader is referred to our previous report.[5] In practice, it is convenient to replace $\overline{u'^2}$, $\overline{v'^2}$, $\overline{w'^2}$ by the kinetic energy $q^2 = (\overline{u'^2} + \overline{v'^2} + \overline{w'^2})/2$ and two measures of the degree of anisotropy $S_{11} = \overline{u'^2} - 2/3\, q^2$, $S_{22} = \overline{v'^2} - 2/3\, q^2$. In all of the following equations, the diffusion terms (second partial derivatives with respect to y) should be understood to be multiplied and divided by $B(y)$ as in Eq. 3.

For steady flow, the governing equations include continuity:

$$\frac{\partial}{\partial x_i} (\rho U_i) = 0 \tag{A-1}$$

the mean momentum equation:

$$\rho U_k \frac{\partial U}{\partial x_k} = - \frac{\partial \bar{p}}{\partial x} - \frac{\partial}{\partial y} (\rho \overline{uv}) + \frac{\partial}{\partial y}\left(\mu \frac{\partial U}{\partial y}\right) + R_u \tag{A-2}$$

and, for the five second-order quantities:

$$\rho U_k \frac{\partial q^2}{\partial x_k} = - \rho \overline{uv} \frac{\partial U}{\partial y} - \rho \xi + 0.2 \frac{\partial}{\partial y}\left[\rho \frac{q^2 v^2}{\xi} \frac{\partial}{\partial y} (q^2 + v^2)\right]$$

$$+ \frac{\partial}{\partial y} \mu \frac{\partial q^2}{\partial y} + (S_{22} - S_{11}) \rho \frac{\partial U}{\partial x} + R_q \tag{A-3}$$

$$\rho U_k \frac{\partial S_{11}}{\partial x_k} = - \frac{14}{33} \rho \overline{uv} \frac{\partial U}{\partial y} - C_E \rho \frac{\xi}{q^2} S_{11} + 0.2 \frac{\partial}{\partial y}\left[\rho \frac{q^2 v^2}{\xi} \frac{\partial}{\partial y} \left(S_{11} - \frac{2}{3} v^2\right)\right]$$

$$+ \frac{\partial}{\partial y} \mu \frac{\partial S_{11}}{\partial y} - \rho \left[\frac{8}{15} q^2 + \frac{2}{33} S_{11} + \frac{1}{33} S_{22}\right] \frac{\partial U}{\partial x} \tag{A-4}$$

- 36 -

$$\rho U_k \frac{\partial S_{22}}{\partial x_k} = \frac{13}{33} \rho \overline{uv} \frac{\partial U}{\partial y} - C_E \rho \frac{\xi}{q^2} S_{22} + 0.2 \frac{\partial}{\partial y} \left[ \rho \frac{q^2 v^2}{\xi} \frac{\partial}{\partial y} (S_{22} - \frac{4}{3} v^2) \right]$$

$$+ \frac{\partial}{\partial y} \mu \frac{\partial S_{22}}{\partial y} + \rho \left[ \frac{8}{15} q^2 + \frac{1}{33} S_{11} + \frac{2}{33} S_{22} \right] \frac{\partial U}{\partial x} . \tag{A-5}$$

$$\rho U_k \frac{\partial \overline{uv}}{\partial x_k} = - \rho \left[ \frac{4}{15} q^2 - \frac{2}{11} S_{11} + \frac{5}{22} S_{22} \right] \frac{\partial U}{\partial y} - C_E \rho \frac{\xi}{q^2} \overline{uv}$$

$$+ 0.4 \frac{\partial}{\partial y} \left[ \rho \frac{q^2 v^2}{\xi} \frac{\partial \overline{uv}}{\partial y} \right] + \frac{\partial}{\partial y} \mu \frac{\partial \overline{uv}}{\partial y} \tag{A-6}$$

$$\rho U_k \frac{\partial \xi}{\partial x_k} = - 1.25 \rho \frac{\overline{uv}}{q^2} \frac{\partial U}{\partial y} \xi - C_{\xi} \rho \frac{\xi^2}{q^2} + 177.6 \rho \frac{v^2 q^2}{y^4}$$

$$+ 0.322 \frac{\partial}{\partial y} \left[ \rho \frac{q^2 v^2}{\xi} \frac{\partial \xi}{\partial y} \right] + \frac{\partial}{\partial y} \mu \frac{\partial \xi}{\partial y} - 1.25 \rho \frac{u^2}{q^2} \frac{\partial U}{\partial x} \xi + R_{\xi} \tag{A-7}$$

where $C_E = \dfrac{1.2 + 12.5 \, \pi/Re_{\Lambda}}{1 + 12.5 \, \pi/Re_{\Lambda}}$ ,

$$C_{\xi} = \frac{\left( 0.288 + 6.6 \, \pi/Re_{\Lambda} + 35 \, \pi^2/Re_{\Lambda}^2 \right)}{(0.4 + 5 \, \pi/Re_{\Lambda})^2}$$

and $Re_{\Lambda}$ is the turbulent Reynolds number $q\Lambda/\nu$, with $\Lambda$ being related to the dissipation rate by

$$\bar{\Phi} = 0.4 \frac{q^3}{\Lambda} + 5 \pi \nu \frac{q^2}{\Lambda^2} = 0.4 \frac{q^3}{\Lambda} (1 + 12.5 \pi/Re_\Lambda) \qquad (A-8)$$

the corresponding equations for enthalpy-related quantaties are:

$$\rho \frac{D\bar{h}}{Dt} = \bar{U}_i \frac{\partial \bar{p}}{\partial x_i} - \frac{\partial}{\partial y} (\overline{\rho v'h'}) + \frac{1}{Pr} \frac{\partial}{\partial y} \left(\mu \frac{\partial \bar{h}}{\partial y}\right) + \mu \left(\frac{\partial U}{\partial y}\right)^2 + \rho \bar{\Phi} \qquad (A-9)$$

$$\rho \frac{\overline{Dh'^2}}{Dt} = -2 \overline{\rho v'h'} \frac{\partial \bar{h}}{\partial y} - C_{T_1} \rho \frac{\bar{\Phi}}{q^2} \overline{h'^2} + 0.40 \frac{\partial}{\partial y} \left(\rho \frac{q^2 v^2}{\bar{\Phi}} \frac{\partial \overline{h'^2}}{\partial y}\right)$$
$$+ \frac{1}{Pr} \frac{\partial}{\partial y} \left(\mu \frac{\partial \overline{h'^2}}{\partial y}\right) \qquad (A-10)$$

$$\rho \frac{D\overline{v'h'}}{Dt} = -\rho v^2 \frac{\partial \bar{h}}{\partial y} - 0.09835 \overline{\rho u'h'} \frac{\partial U}{\partial y} - C_{T_2} \rho \frac{\bar{\Phi}}{q^2} \overline{v'h'}$$
$$+ 0.80 \frac{\partial}{\partial y} \left(\rho \frac{q^2 v^2}{\bar{\Phi}} \frac{\partial}{\partial y} \overline{v'h'}\right) + \frac{1}{Pr} \frac{\partial}{\partial y} \left(\mu \frac{\partial \overline{v'h'}}{\partial y}\right) \qquad (A-11)$$

$$\rho \frac{D\overline{u'h'}}{Dt} = -0.3989 \overline{\rho v'h'} \frac{\partial U}{\partial y} - \rho \overline{uv} \frac{\partial \bar{h}}{\partial y} - C_{T_2} \rho \frac{\bar{\Phi}}{q^2} \overline{u'h'}$$
$$+ 0.40 \frac{\partial}{\partial y} \left(\rho \frac{q^2 v^2}{\bar{\Phi}} \frac{\partial \overline{u'h'}}{\partial y}\right) + \frac{1}{Pr} \frac{\partial}{\partial y} \left(\mu \frac{\partial \overline{u'h'}}{\partial y}\right) \qquad (A-12)$$

- 38 -

where $C_{T_1} = \dfrac{0.8 + 7.5\,\pi/Re_\Lambda}{1 + 12.5\,\pi/Re_\Lambda}$

$$C_{T_2} = \dfrac{1.165 + 12.5\,\pi/Re_\Lambda}{1 + 12.5\,\pi/Re_\Lambda}.$$

The terms $R_u$, $R_h$, $R_q$, and $R_\phi$ contain the effect of roughness on the boundary layer. For the mean velocity and enthalpy equations, $R_u$ and $R_h$ were presented in Eqs. (1) and (2) in Section II, the other two terms are source terms for kinetic energy and dissipation, describing the fluctuations introduced in the wakes of elements. For the fully turbulent boundary layers considered in this study, these terms are generally small compared to the natural turbulence production terms. As described in Ref. 5, the terms used are:

$$R_q = 0.04\rho U^3 D/\ell^2 \qquad\qquad (A-13)$$

$$R_\phi = 0.04\rho U^3 \nu/D\ell^2 \qquad\qquad (A-14)$$